

Strategies for Finding Training Snapshots for the Hyperreduction Method ECSW in Magnetodynamic Systems

Johannes Maierhofer^{1,*} and Daniel J. Rixen¹

¹ Technical University of Munich, TUM School of Engineering and Design, Chair of Applied Mechanics

Model order reduction for nonlinear magnetodynamic systems can be approached, using hyperreduction methods such as DEIM and ECSW. Typical for this methods is the data-driven approach. Therefore, the full order model has to be solved several times to generate a sufficient data basis to extract all the necessary information for the reduced order model.

Hyperreduction is a two step process. First, a new (much smaller) solution space needs to be found where the model is projected into without significant loss of information. Second, a subset of elements has to be chosen and weighted such that the hyperreduced model preserves the result in an appropriate manner.

This contribution focuses on the Energy Conserving Sampling and Weighting (ECSW) method and shows different heuristic strategies to find appropriate training snapshots.

© 2023 The Authors. *Proceedings in Applied Mathematics & Mechanics* published by Wiley-VCH GmbH.

1 Introduction

The calculation of low frequency electrodynamic (= magnetodynamic) systems using the Finite Element Method (FEM) is common practice. Due to the skin-effect of the Eddy currents, the mesh size needs to be very small for the boundary areas of the geometry. This leads to a high computational effort, especially as the system is non-linear. The non-linearity arises from the magnetic saturation of iron materials. The discretized equation is first order and of the following structure:

$$M\dot{u} + g(u) = f \quad (1)$$

The unknown u represents the vector potential of the magnetic field from which the magnetic field density and the Eddy-currents are calculated in a postprocessing step. The magnetic mass M and the magnetic stiffness g depend on the material properties conductivity and the non-linear permeability (see fig. 1) respectively. As excitation, a controlled current f is applied. The equation is time integrated using a simple Euler backward scheme. A detailed derivation of the magnetodynamic equation and discretization can be read in [2].

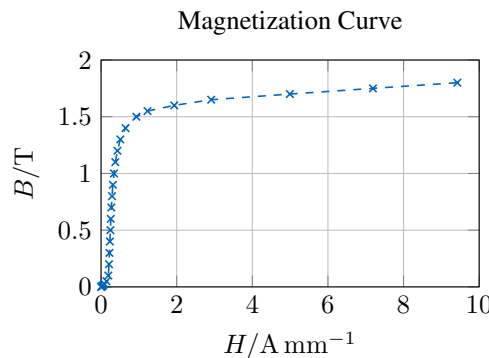


Fig. 1: Non-linear material behavior with spline interpolation between the measured values of the data sheet.

1.1 Model Order Reduction

To reduce the high computational costs, model order reduction techniques are desirable tools in the case when many, or fast simulations are needed. In this case, the so-called hyperreduction method *Energy Conserving Sampling and Weighting* (short ECSW) is applied. The class of hyperreduction methods are characterized by their two step reduction structure. The first step is a projection step to a (much) smaller space where the solution is assumed to be expressed in within a certain tolerance. A loss of information and therefore of precision is not avoidable.

As the projection does not reduce the effort of evaluating the non-linear term over all elements, the second reduction step considers only a subset of elements to evaluate and weights their contribution such that a criterion (depending on the method)

* Corresponding author: e-mail j.maierhofer@tum.de



This is an open access article under the terms of the Creative Commons Attribution-NonCommercial License, which permits use, distribution and reproduction in any medium, provided the original work is properly cited and is not used for commercial purposes.

is fulfilled. This second, so-called *hyper*-reduction step leads to a remarkably reduced model. But again, this second reduction is also an approximation and introduces some error.

1.2 Training Snapshots

Arising from the two step approach of the hyperreduction, there are two reduction steps where the parameters need to be found to achieve a sufficient good result. The strategy shown here is simulation based (= data-driven), which means that a full-order time-integration simulation is performed for a certain training trajectory of the load (i.e. the current in the coil). The full-order solution vectors of each time step are called the training snapshots. Truncating a singular-value-decomposition on a set of training snapshots results in the smaller solution space for the projection. Second, a set of training snapshots is used to select the elements for the ECSW-method.

1.3 Possible strategies for selecting the training snapshots

From the previously shown use of the training snapshots, different strategies for generating and selecting the training snapshots arise. Due to the expenses in generation of the training snapshots by full-order time integration, a few rules of best practice can be stated directly:

- Make use of every snapshot generated.
- Choose a trajectory that captures the system's behavior with a minimum of time steps.

2 Example

As an example for this contribution, the *TEAM10* model from the *Compumag*-Society is used. The structure was invented in the 1990s to serve as a benchmark system for the different finite element formulations and code implementations. Also, the example was set up in the lab and highly sophisticated measurements were performed to check the simulations' results with. The summary of the results can be found in [4] and are used here as the reference.

The system fig. 2 is dominated by a copper ring (depicted in orange) and three thin sheet metal plates. Two c-shaped plates are arranged symmetrically around the vertical middle plate. The whole structure is surrounded by an air box to allow the magnetic- and electric field to propagate between the solid parts.

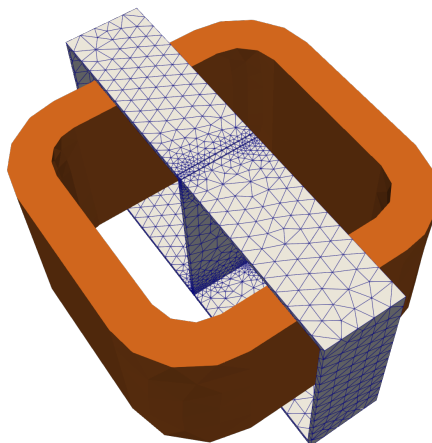


Fig. 2: TEAM10 benchmark example, showing the mesh for the thin sheet metal plates. The whole system is encapsulated in an air box which is not shown here.

2.1 Reference Solution

To proof the simulation environment, the reference trajectory is applied to the system and the results are compared with the official measurements of the benchmark report. The comparison in fig. 3 shows a good agreement of the magnetic field density in all of the three test locations. The Eddy-currents show some discrepancies for the time range of 25 ms to 75 ms. This was traced back to the fact that the steel plates are only meshed with one layer of elements. For the sake of this contribution this wasn't an issue and the mesh was not refined. The full-order model has 462 308 dofs and 89 534 elements. The element order is 2, the timestep size $t = 0.002$ s.

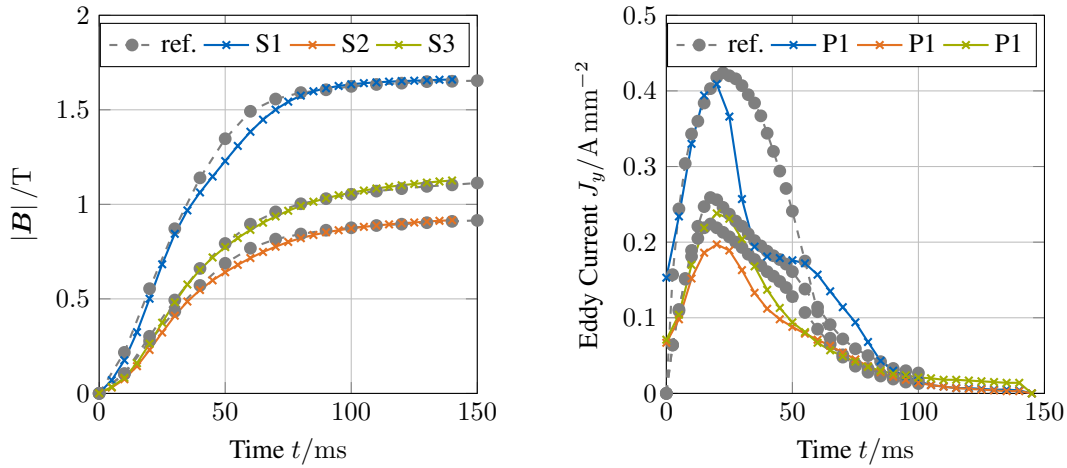


Fig. 3: Comparison of the official benchmark measurements and the simulation results at the specified positions S1-3 and P1-3. The Eddy-currents show some discrepancies which can be traced back to relatively low mesh density in the middle plate.

2.2 Training Trajectories

Training load trajectories have to fulfill certain constraints. The maximum presentable frequency of the system is determined by the mesh size and the conductivity of the material. The phenomena of skin-effect describes the depth up to which the Eddy-currents occur in significant amount due to the change rate in the magnetic field density. The element size has to be at least in the same order of magnitude.

The first excitation function forms a smooth step:

$$I_1(t) = \begin{cases} 0 & (t < 0) \\ I_m(1 - e^{-\frac{t}{\tau}}) & (t \geq 0) \end{cases} \quad \begin{matrix} I_m & 5.64 \text{ A} \\ \tau & 0.05 \text{ s} \end{matrix} \quad (2)$$

The second excitation function forms an impulse:

$$I_2(t) = I_m e^{-\frac{(t-m)^2}{2a^2}} \quad I_m = 5.64 \text{ A}, \quad m = 0.05 \text{ s}, \quad a = 0.01 \text{ s} \quad (3)$$

The third excitation function forms a sine:

$$I_3(t) = I_m \sin(2\pi ft) \quad I_m = 5.64 \text{ A}, \quad f = 10 \text{ Hz} \quad (4)$$

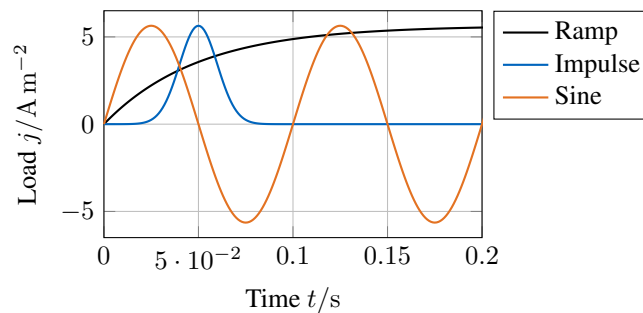


Fig. 4: The three excitation trajectories used throughout the study.

3 Tools

To quantify data driven approaches, a few tools are introduced here. They give insight into the achievable solutions during the model order reduction process. Also the quality of the final result can be measured relative to the full-order model.

3.1 Singular Value Decomposition

To find a basis that spans the subspace which is consumed by the solution of the training simulation, a proper orthogonal decomposition (short POD) of the training snapshots is performed using the singular value decomposition (short SVD). The

singular values of the SVD show the importance of the left sided vectors of the decomposition. The decay of the singular values gives a hint how much of the solution lives within the most important directions. A strong decay indicates strong first modes. But for achieving equally good subspaces, it is not sufficient to truncate different PODs to the same level of singular value, as they are not independent of the configuration space. That means the singular values are not comparable from training set to training set in an absolute manner.

3.2 Subspace Angles

As the generation of the subspace where the system is projected into is a data driven approach by performing an svd on the training snapshots, different training simulations could lead to different subspaces. Depending on the unknown trajectory that will be simulated with the reduced order model, the subspace could be more or less sufficient to represent the true solution. To compare two subspaces without the dependence on their representing vectors, the concept of *subspace angles* is introduced. [5] For the exact algorithm, the interested reader is hinted to [5] or other sources [1]. The subspace angles between two subspaces \mathcal{S}_∞ and \mathcal{S}_ϵ are defined in eq. (5), where the maximum angle Θ_i between the vector $\mathbf{v}_i \in \mathcal{S}_\infty$ and $\mathbf{w}_i \in \mathcal{S}_\epsilon$ is found.

$$\cos \Theta_i = \max \mathbf{v}_i^T \mathbf{w}_i, \quad \mathbf{v}_i^T [\mathbf{v}_1, \dots, \mathbf{v}_{i-1}] = 0, \quad \mathbf{w}_i^T [\mathbf{w}_1, \dots, \mathbf{w}_{i-1}] = 0 \quad (5)$$

To give the two extreme situations as illustration: Any vector $\mathbf{v}_i \in \mathcal{S}_1$ is orthogonal to any other vector $\mathbf{w}_i \in \mathcal{S}_2$, resulting in $\Theta = 90^\circ$. Two subspaces are identical, if all subspace angles are $\Theta = 0$.

As the size of subspaces can be different, the concept of subspace angles still gives valuable results. It can show how well the smaller subspace is included in the wider one.

3.3 Relative Error

The relative error compares resulting values with reference values (i.e. the full-order model results) over all timesteps. The relative error is applicable to local or global measures. An example for a local measure is the relative error of the B-field at one specific point. An example for a global measure is the total magnetic energy in the system. Concluding, the relative error is a measure to quantify the reduced order model, whereas the subspace angles and the singular values just give insights but the consequences on the quality of the ROM can't directly be drawn.

4 Results

Three training simulations differing in their excitation function are performed. All simulations are performed using the same settings $\Delta t = 0.002$ s, $n = 50$ timesteps. The excitation functions are: ramp, impulse, and sine.

4.1 Generation of Solution Subspace

The three resulting snapshot collections are used to compute one POD per experiment. The singular value decay and the subspace angles referenced to the ramp excitation are plotted in fig. 5. The ramp excitation leads to the fastest decay of

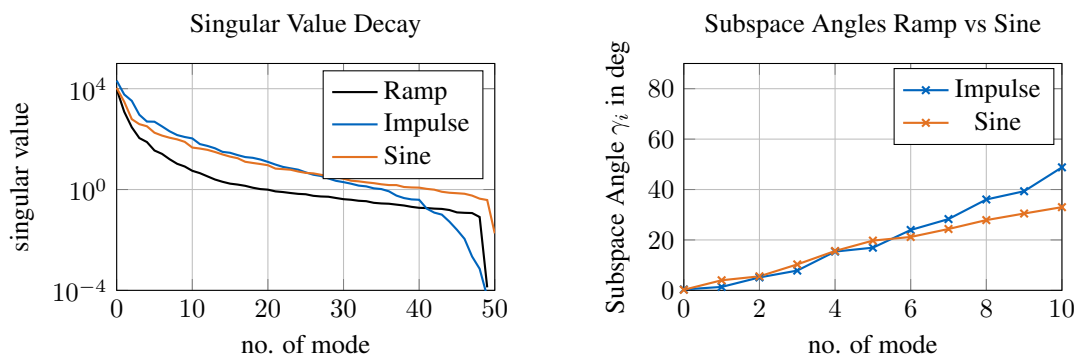


Fig. 5: Left: Decay of the singular values for each training simulation. Right: Subspace angles of the Impulse and Sine generated subspaces in reference to the Ramp experiment.

singular values which indicates that less left vectors can represent the major behavior of the solution. The impulse and sine excitation show a very similar pattern. Regarding the subspace angles, the subspaces show quite some deviations even in the first 10 modes. One can not say that one subspace embraces the other fully. The consequences on the final reduced model can't be estimated for now.

4.2 Selection of Evaluation Elements

The training snapshots for the element selection process (algorithm sNNLS) are chosen to be the same as for generating the subspace. The sNNLS-Algorithm features a tolerance τ which sets the precision of the weighted result in relation to the evaluation of all elements.

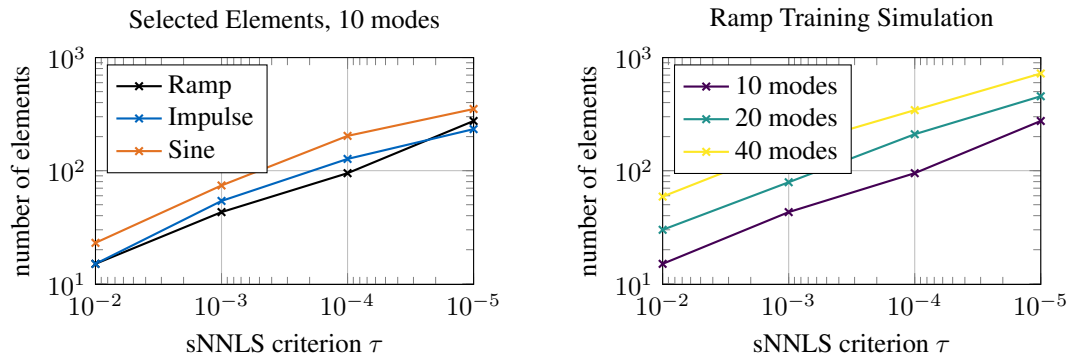


Fig. 6: Left: Number of elements over the tolerance criterion τ for the three training sets. Right: Influence of subspace size

The left plot shows the difference in selected numbers of elements due to different training simulations. Again, the ramp training snapshots seem to be more valuable as with the use of them, the tolerance is hit with less elements than the comparison partners. The right plot indicates that bigger subspaces (i.e. higher number of considered modes) lead to a higher number of selected elements. The shown number of elements arise from the ramp training snapshots.

One exemplary configuration leads to the element distribution shown in fig. 7.

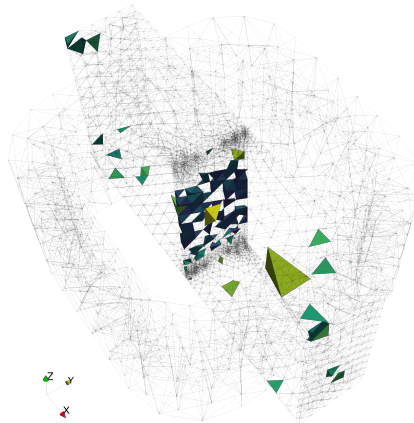


Fig. 7: Selected elements for the ECSW method. A concentration is seen in the areas of high Eddy-currents. The color represents the weighting factor.

4.3 Relative Error

Next, the time integration of the reduced order model is performed again for all three excitation functions and compared against each other. Comparing the results of different hyperreduced models against their full-order reference solution leads to the kivi diagram in fig. 8. Each ray represents a relative error measure (local and global). The shorter the circular path, the better.

For the interpretation of the relative error numbers, one has to keep in mind that the reduced order models are constructed to be as small as possible to give at least reasonable results. This leads to quite big relative errors which would not be usable in good practice. Two statements can be drawn from fig. 8. First: The reduced order model represents its own training simulation the best. This was expectable as this is exactly how the model was trained. This is often called the onboard validation. Second: The impulse trained model is not capable of reproducing the ramp or sine trajectory and is therefore not even plotted in the graph.

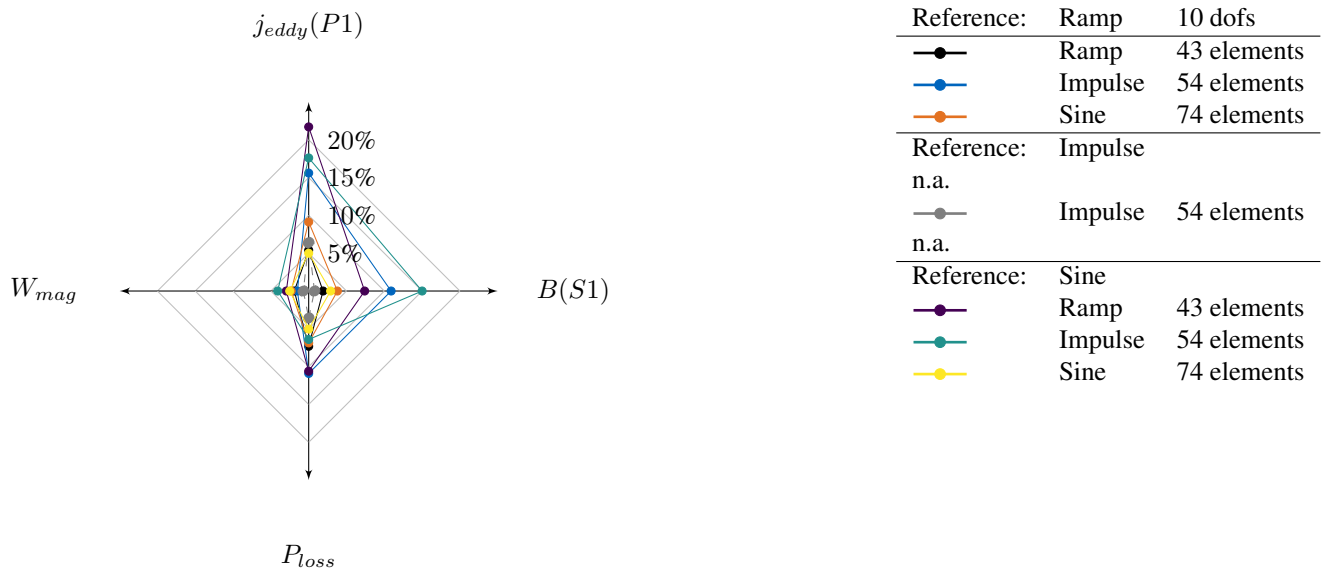


Fig. 8: Relative Error, evaluated for different quantities (global energy W_{mag} and power loss P_{loss} , local field quantities B and A). The graph contains the three combination groups of where the reference is the full simulation respectively.

5 Conclusion

The contribution shows the big potential of hyperreduction methods like ECSW for magnetodynamic systems. To find efficient training simulations, three different approaches are proposed and compared using various quantification methods. The results show some obvious behavior (the more elements, the better the hyperreduction result) which seem very robust. Also, finding an appropriate subspace was possible using all three training simulations. The element selection also depends on the training snapshots. Here, some differences occurred that lead even to very bad reduced order models for the impulse training. However it was not possible to find a measure to determine bad reduced order models in advance.

A showcase how to use the gained knowledge in the process of model order reduction using the ECSW-method for monitoring processes is given in [3].

A completely different approach to find the reduction parameter sets would be the branch of simulation-free approaches. There, the idea is to exploit the system properties in form of eigenvalue problems or use different quasi-static solutions. This has the advantage that the full-order system never has to be computed.

Finally, it stays a difficult task to classify the reduction quality for nonlinear models beforehand. Although tools like the subspace angles give more insight the reduction basis, the interpretation keeps open until more case studies bring higher confidence.

Acknowledgements Open access funding enabled and organized by Projekt DEAL.

References

- [1] Gene H. Golub and Charles F. Van Loan. *Matrix Computations*. Johns Hopkins University Press, 2013. ISBN: 9781421408590.
- [2] Johannes Maierhofer and Daniel J. Rixen. “Model Order Reduction using Hyperreduction Methods (DEIM, ECSW) for Magnetodynamic FEM Problems”. In: *Finite Elements in Analysis and Design* (2022).
- [3] Johannes Maierhofer et al. “Multiphysical Simulation, Model Order Reduction (ECSW) and Experimental Validation of an Active Magnetic Bearing”. In: *Actuators 11.6* (June 2022), p. 169. DOI: 10.3390/act11060169.
- [4] Takayoshi Nakata, Norio Takahashi, and Koji Fujiwara. “Summary of results for benchmark problem 10 (Steel plates around a coil)”. In: *COMPEL - The international journal for computation and mathematics in electrical and electronic engineering 11.3* (Mar. 1992), pp. 335–344. DOI: 10.1108/eb010096.
- [5] Johannes B Rutzmoser, Fabian M Gruber, and Daniel J Rixen. “A Comparison on Model Order Reduction Techniques for Geometrically Nonlinear Systems Based on a Modal Derivative Approach Using Subspace Angles”. In: *Proceedings of the 11th International Conference on Engineering Vibration*. Sept. 2015.